

The Pan-Pacific Planet Search. I. A Giant Planet Orbiting 7 CMa

Robert A. Wittenmyer¹, Michael Endl², Liang Wang³, John Asher Johnson⁴, C.G. Tinney¹,
S.J. O'Toole⁵

rob@phys.unsw.edu.au

ABSTRACT

We introduce the Pan-Pacific Planet Search, a survey of 170 metal-rich Southern hemisphere subgiants using the 3.9m Anglo-Australian Telescope. We report the first discovery from this program, a giant planet orbiting 7 CMa (HD 47205) with a period of 763 ± 17 days, eccentricity $e = 0.14 \pm 0.06$, and $m \sin i = 2.6 \pm 0.6 M_{\text{Jup}}$. The host star is a K giant with a mass of $1.5 \pm 0.3 M_{\odot}$ and metallicity $[\text{Fe}/\text{H}] = 0.21 \pm 0.10$. The mass and period of 7 CMa b are typical of planets which have been found to orbit intermediate-mass stars ($M_* > 1.3 M_{\odot}$). *Hipparcos* photometry shows this star to be stable to 0.0004 mag on the radial-velocity period, giving confidence that this signal can be attributed to reflex motion caused by an orbiting planet.

Subject headings: planetary systems – techniques: radial velocities – stars: individual (HD 47205)

1. Introduction

Nearly 20 years of concerted radial-velocity monitoring of solar-type main-sequence stars has unveiled a fascinating diversity of planets and planetary system configurations. From the many hundreds of planets now characterised, the observational evidence is mounting

¹Department of Astrophysics, School of Physics, University of NSW, 2052, Australia

²McDonald Observatory, University of Texas at Austin, 1 University Station C1400, Austin, TX 78712, USA

³Key Laboratory of Optical Astronomy, National Astronomical Observatories, Chinese Academy of Sciences, A20 Datun Road, Chaoyang District, Beijing 100012, China

⁴Department of Astrophysics, California Institute of Technology, MC 249-17, Pasadena, CA 91125, USA

⁵Australian Astronomical Observatory, PO Box 296, Epping, 1710, Australia

for several interesting relationships between the properties of planets and their host stars. Among these are: (1) giant planet occurrence is positively correlated with stellar metallicity (Fischer & Valenti 2005) and mass (Johnson et al. 2010a; Endl et al. 2006), (2) short-period “Super-Earths” with $m \sin i < 10 M_{\oplus}$ are about an order of magnitude more common than close-in giant planets (Howard et al. 2010; Wittenmyer et al. 2011), and (3) planet mass is positively correlated with host star mass (Bowler et al. 2010).

Most of the stars which have been targeted by radial-velocity surveys have masses which fall in the range 0.7-1.3 M_{\odot} (Johnson 2007; Valenti & Fischer 2005). This is a consequence of the technical requirements of Doppler exoplanetary detection, which demand that stars be cool enough to present an abundance of spectral lines, and rotate slowly enough that their absorption lines are not significantly broadened by rotation. Stars of lower mass (e.g. M dwarfs) are intrinsically faint in the optical, making the acquisition of high signal-to-noise spectra extremely expensive in telescope time (Endl et al. 2006). Main sequence stars of higher mass have few usable absorption lines (due to their high temperatures), and also tend to be fast rotators ($v \sin i > 50 \text{ km s}^{-1}$; Galland et al. 2005) due to their youth. In addition, the shorter main-sequence lifetimes of higher-mass stars means that they will preferentially be observed at younger ages. Stars earlier than about F7 also have much shallower convection zones, and so do not experience the magnetic braking which slows the rotation of later-type (lower-mass) stars. As a result, only the most massive planets can be detected orbiting A and F dwarfs. It is only recently that a significant number of planetary systems have been discovered orbiting intermediate-mass stars ($M_* > 1.3M_{\odot}$). These stars have proven to be a fertile hunting ground for interesting planetary systems, such as the 4:3 mean-motion resonant planets orbiting HD 200964 (Johnson et al. 2011). Now, some headway is beginning to be made in addressing the crucial question of how planet formation depends on stellar mass (Bowler et al. 2010; Johnson et al. 2010a; Sato et al. 2010). A number of surveys are seeking to expand our knowledge of planetary systems orbiting stars more massive than the Sun, e.g. Setiawan et al. (2003); Hatzes et al. (2005); Sato et al. (2005); Johnson et al. (2006b); Döllinger et al. (2007); Niedzielski et al. (2009). These surveys are exploiting the advantage wrought by stellar evolution: as stars evolve off the main sequence into subgiants and giants, their atmospheres expand and cool, making precision Doppler velocity measurements possible due to an abundance of narrow spectral lines.

The well-known planet-metallicity correlation (Gonzalez 1999; Fischer & Valenti 2005), whereby main-sequence stars with higher metal content are more likely to host planets, has come under some scrutiny. Analysis of the metallicities of planet-hosting giant stars by Schuler et al. (2005) showed that the giant star planet hosts were significantly more metal-poor than their main-sequence counterparts. Pasquini et al. (2007) have also argued that the planet-metallicity correlation does not apply for evolved stars. They propose that this is evi-

dence for a “pollution” scenario, in which main-sequence stars hosting planets appear metal-rich because they have accreted material from the protoplanetary disk (Murray & Chaboyer 2002). When a star evolves off the main sequence, the convective zone increases in size by about a factor of 35 (Pasquini et al. 2007). If the high metallicities observed in planet hosts are due to pollution, this expansion of the convective zone will significantly dilute the extent of that pollution, and the subgiant’s photosphere would return to its “birth” metallicity. Hence, one would *not* expect a significant correlation between metallicity and planet frequency for subgiants.

However, the importance of planet pollution was downplayed even by the authors who proposed it, as they felt it should play only a minor role in shaping the planet-metallicity correlation seen in dwarf stars. Further, Valenti & Fischer (2008), Johnson et al. 2010a, Takeda et al. (2007) and others found no evidence of a decreasing planet-metallicity correlation among F dwarfs, subgiants or K giants. The sample of K giants studied by Pasquini et al. (2007) had a limited metallicity range, with $[\text{Fe}/\text{H}] < +0.2$. Examination of the form of the planet-metallicity correlation of Fischer & Valenti (2005) and Johnson et al. (2010a) shows that, for small numbers of stars, the correlation over this metallicity range would look approximately flat.

One way to test this is to search for planets around a sample of evolved stars that are unambiguously metal rich. Sandage et al. (2003) pointed out that stars on the red-edge of the subgiant branch represent such a population. Here, we introduce a new Southern Hemisphere survey, the “Pan-Pacific Planet Search,” which uses the 3.9-metre Anglo-Australian Telescope (AAT) to search for planets among these evolved, metal-rich stars to test for evidence of planet pollution.

In this paper, we present the first result from this new survey: the detection of a 2.6 M_{Jup} planet orbiting the nearby evolved star HD 47205. In Section 2, we introduce the Pan-Pacific Planet Search and give a complete target list for the survey. Section 3 describes the observational data and gives the stellar parameters for 7 CMa. In Section 4, we detail the orbit-fitting process and present the planetary parameters. Finally, in Section 5 we discuss the further implications of this discovery.

2. The Pan-Pacific Planet Search

2.1. Survey Strategy and Target Selection

The Pan-Pacific Planet Search (PPPS) originated as a Southern hemisphere extension of the established Lick & Keck Observatory survey for planets orbiting Northern “retired A

stars” (Johnson et al. 2006b, 2007, 2010a). This program is using the 3.9m Anglo-Australian Telescope (AAT) to observe a metal-rich sample of Southern Hemisphere subgiants. We have selected 170 Southern stars with the following criteria: $1.0 < (B - V) < 1.2$, $1.8 < M_V < 3.0$, and $V < 8.0$. By requiring $(B - V) > 1$, we extend the red limit of the Johnson et al. (2006b) survey to the colours that stellar models indicate will be dominated by metal-rich subgiants (Girardi et al. 2002). This aims to deliver improved planetary detection statistics at $[\text{Fe}/\text{H}] > 0.0$. In light of the observed positive correlation between stellar metallicity and planet occurrence, this should also deliver a roughly equivalent number of planetary detections to that obtained at Lick and Keck, though for metal-rich hosts. At the same time, by requiring $M_V > 1.8$, we exclude giant-branch stars, as these have significant intrinsic velocity noise (“jitter”) due to random convective motion and pulsations (Saar et al. 1998; Wright 2005) – typically about 20 m s^{-1} (Hekker et al. 2006). Our target list includes about 30 stars from the Lick survey; this overlap will serve as a check on the systematics between the two telescopes. Together, the three telescopes are observing more than 600 stars. The complete PPS target list is given in Table 1.

Observing time is scheduled such that each target should receive 4–6 observations per year. This strategy would appear to reduce the probability of detecting shorter-period planets ($P \lesssim 50$ days), which require more densely-sampled observations in continuous blocks of time (O’Toole et al. 2009a,b; Vogt et al. 2010). However, we note that the same scheduling has been used in the Lick and Keck survey, which has detected the $P = 6.5$ day planet orbiting HD 102956 (Johnson et al. 2010c). By employing this strategy, we are able to target more stars with a fixed amount of observing time, which should increase the probability of detecting the types of planets which are known to orbit nearly 20% of these types of stars (Johnson et al. 2010a).

2.2. Observations and Data Reduction

PPS Doppler measurements are made with the UCLES echelle spectrograph (Diego et al. 1991) at the 3.9-metre Anglo-Australian Telescope (AAT). UCLES achieves a resolution of 45,000 with a 1-arcsecond slit. An iodine absorption cell provides wavelength calibration from 5000 to 6200 Å. The spectrograph point-spread function and wavelength calibration are derived from the iodine absorption lines embedded on every pixel of the spectrum by the cell (Valenti et al. 1995; Butler et al. 1996). The result is a precision Doppler velocity estimate for each epoch, along with an internal uncertainty estimate, which includes the effects of photon-counting uncertainties, residual errors in the spectrograph PSF model, and variation in the underlying spectrum between the iodine-free template, and epoch spectra

observed through the iodine cell. The photon-weighted mid-time of each exposure is determined by an exposure meter. All velocities are measured relative to the zero-point defined by the template observation. Velocities are obtained using the *Austral* code as first discussed in Endl et al. (2000). *Austral* is a proven Doppler code which has been used by the McDonald Observatory planet search programs for nearly 10 years (e.g. Endl et al. 2004, 2006; Wittenmyer et al. 2009).

Observations for the PPS began at the Anglo-Australian Telescope in 2009 February. Since its inception, the program has received 20 nights per year, of which approximately 50% have resulted in usable data. We aim for a signal-to-noise (S/N) of 100 at 5500 Å per spectral pixel each epoch, resulting in exposure times ranging from 100 s up to a maximum of 20 minutes.

We have observed 7 CMa on 21 epochs, and an iodine-free template observation was obtained on 2010 Jan 30. Since 7 CMa is an extremely bright star, exposure times ranged from 100 to 500 s, with a resulting S/N of ~ 200 -300 per pixel each epoch. The data span a total of 917 days, and have a mean internal velocity uncertainty of 6.5 m s^{-1} .

3. Stellar Parameters of 7 CMa

7 CMa (=HD 47205, HIP 31592) is one of the brightest stars in the PPS survey ($V = 3.95$). In addition, it is accessible from most sites in both hemispheres (RA: 06 36 41.038, Dec: -19 15 21.17), and so it has been well-studied. Table 2 summarises the physical parameters of this star. We have used our iodine-free template spectrum to derive spectroscopic stellar parameters, using methods described fully in Wang et al. (2011). In brief, 7 CMa is an evolved, somewhat metal-rich ($[\text{Fe}/\text{H}] \sim 0.2$), intermediate-mass star ($1.52 M_{\odot}$) with a low level of activity. *Hipparcos* observations indicate that it is photometrically stable, with a median *Hipparcos* magnitude of 4.1200 ± 0.0004 (van Leeuwen 2007; Perryman et al. 1997).

4. Orbit Fitting and Planetary Parameters

The AAT data show a root-mean-square (RMS) scatter of 29.5 m s^{-1} about the mean velocity. Visual investigation of the data after two years of observation revealed a clear sinusoidal trend. Due to the relative paucity of data points ($N = 21$) compared to typical radial-velocity planet detections ($N \gtrsim 40$), the traditional periodogram approach does not produce reliable estimates of statistical significance. Rather, since the periodic signal is readily apparent by eye, we used a genetic algorithm (Charbonneau 1995) to determine Keplerian

orbital parameters. Those parameters were then used as initial inputs for a standard least-squares fitting routine. Our previous experience with genetic algorithms (Cochran et al. 2007; Tinney et al. 2011) has shown that the solution “evolves” quite rapidly toward a sharp χ^2 minimum when brought to bear on data containing a real and coherent Keplerian signal. Indeed, with an allowed period range of 600–800 days, the algorithm converged on a solution with a period of 769 days and a small eccentricity $e = 0.23$. We then used the *GaussFit* code (Jefferys et al. 1987) to obtain a Keplerian model fit for the planet. For the final orbit fitting, we added 5 ms^{-1} of jitter in quadrature to the internal uncertainties of the data shown in Table 4. The jitter estimate of 5 ms^{-1} is derived from Johnson et al. (2010a). In that work, 382 velocity measurements from 72 stable stars in the Lick and Keck survey of “retired A stars” were used to make an empirical jitter estimate which was then applied to the seven planet-host stars described therein. It would be ideal to estimate jitter for PPPS stars using the same methodology, but at this time, we have insufficient data on radial-velocity stable stars to make a statistically meaningful estimate. This is due to the short time baseline (2.5 yr) and limited available data on a smaller number of stars in the PPPS as compared to the well-established Lick & Keck survey. However, we consider the 5 ms^{-1} jitter estimate to be a reasonable approximation for PPPS targets due to the similarity in physical properties to the Johnson et al. (2010a) sample. We also note that there is substantial ($\gtrsim 50\%$) uncertainty in the estimation of radial-velocity jitter (Wright 2005).

Using a stellar mass of $1.52 \pm 0.30 M_{\odot}$, we estimate the minimum mass $m \sin i$ to be $2.6 \pm 0.6 M_{\text{Jup}}$. The fit is shown in Figure 1 and the planetary parameters are given in Table 3. The residuals of the fit show no evidence for additional signals (Figure 3). As a further test of the veracity of the planet fit, we used the “scrambled velocity” approach of Marcy et al. (2005). This technique serves to test the null hypothesis that the observed velocity variation is attributable to noise. For this test, we scramble the velocities amongst the observation epochs, creating 5000 shuffled data sets. Then, we perform the same least-squares Keplerian orbit-fitting on the shuffled data and log the resulting best-fit χ^2 . The results of these trials are shown in Figure 2 – not one of the scrambled data sets achieved a better χ^2 than the planet fit to our original data. We thus conclude that there is a less than 0.02% probability that the detected signal arose by chance from noise.

5. Discussion

5.1. Testing the Planet Hypothesis

Since many K giants have intrinsic radial-velocity variations with periods of hundreds of days (Hekker et al. 2008), it is prudent for us to further examine the planet hypothesis for

7 CMa to ensure that the observed velocity variations are not associated with known activity and rotational cycles. The first and simplest test is to combine the available estimates of the star’s radius and $v \sin i$ minimum rotational velocity to obtain a maximum rotation period. Using the values for these quantities given in Table 2, this yields a maximum $P_{rot} = 116$ days (for $v \sin i = 1.0 \text{ km s}^{-1}$, Massarotti et al. 2008). Unfortunately, neither estimate of $v \sin i$ has an uncertainty, but if we apply a typical uncertainty of 1 km s^{-1} , then maximum rotation periods shorter than 776 days fall within the 1σ range.

For a spotted star, the rotation period can be deduced from photometry. A periodogram of the *Hipparcos* photometry (after removing one outlier which was more than 1 magnitude discrepant) is shown in Figure 4. Two peaks are evident at periods of 12.2 and 103.7 days. We estimate the false-alarm probability using the bootstrap randomization method (Kürster et al. 1997). The bootstrap method randomly shuffles the observations while keeping the times of observation fixed. The periodogram of this shuffled data set is then computed and its highest peak recorded. From 10,000 such realizations, we find a false-alarm probability of 2.5% for the peak at 12.2 days, and 3.2% for that at 103.7 days. At the 763-day period of the candidate planet, the bootstrap false-alarm probability is 98.7%. The amplitude of the photometric variations for either of the two marginally significant periods is $20 \pm 6 \times 10^{-4}$ mag. In any case, if these small photometric variations are due to the star’s rotation, their periodicities are clearly well-separated from that of the candidate planet.

One can argue that the absence of significant variations in the *Hipparcos* photometry on the 763-day period is not a complete refutation of the starspot hypothesis. Stars have activity cycles, and so there is the possibility that the activity of 7 CMa was at a minimum during the *Hipparcos* observations (20 years before the radial-velocity observations), but is now at a maximum which, if the rotation period were as long as ~ 763 days, could mimic the signal of an orbiting planet. Line bisector analysis is a fairly common technique used by some planet-search programs (e.g. HARPS) to make sure a signal is not due to stellar activity. Such analysis has the advantage of being contemporaneous with the velocity measurements. We note that for the radial-velocity programs using AAT/UCLES, spectra are of relatively low resolution ($R = 45,000$) and nearly all of the usable spectral range is superimposed with iodine lines. We have computed the bisector velocity spans for 8 strong unblended lines redward of the iodine region. The results are shown in Figure 5; each point represents the mean bisector velocity span of 8 lines, and its uncertainty is the standard deviation about the mean value. While the uncertainties are large, it is evident from Figure 5 that the bisector velocity spans are uncorrelated with the radial velocities. Furthermore, the right panel of Figure 5 shows a periodogram of the bisector velocity spans, which also indicates no periodicity near the 763-day period of the planet. These independent lines of evidence thus lead us to conclude that the radial-velocity variations observed in 7 CMa are attributable

not to an intrinsic stellar process, but to an orbiting giant planet.

5.2. Conclusions

Using the Anglo-Australian Telescope, we have begun a Southern hemisphere search for planets orbiting evolved, intermediate-mass stars. Our Pan-Pacific Planet Search team members are based in Australia, China, and the US; we now report the first planet detection from our ongoing survey. There is an emerging trend that planets orbiting intermediate-mass stars tend to have higher masses and longer periods than planets orbiting solar-mass stars (Bowler et al. 2010; Johnson et al. 2010b). With a period of 2.1 years and a minimum mass of $2.6 M_{\text{Jup}}$, 7 CMa b is quite similar to other planets known to orbit intermediate-mass stars. Figure 6 shows the mass and period distribution of all radial-velocity detected planets known to orbit stars with $M_* > 1.3M_{\odot}$, with 7 CMa b plotted as a large filled triangle. Given the abundance of planets with $P \gtrsim 2$ yr known to orbit these types of stars, we anticipate that 7 CMa b is the first of many planet detections to come from the PPPS.

We gratefully acknowledge the UK and Australian government support of the Anglo-Australian Telescope through their PPARC, STFC and DIISR funding; STFC grant PP/C000552/1, ARC Grant DP0774000 and travel support from the Australian Astronomical Observatory. RW is grateful to the Chinese Academy of Sciences for the support of his stay in Beijing. RW is supported by a UNSW Vice-Chancellor’s Fellowship.

We thank the ATAC for the generous allocation of telescope time which facilitated this detection. This research has made use of NASA’s Astrophysics Data System (ADS), and the SIMBAD database, operated at CDS, Strasbourg, France. This research has made use of the Exoplanet Orbit Database and the Exoplanet Data Explorer at exoplanets.org.

REFERENCES

- Bowler, B. P., et al. 2010, *ApJ*, 709, 396
- Butler, R. P., Marcy, G. W., Williams, E., McCarthy, C., Dosanjuh, P., & Vogt, S. S. 1996, *PASP*, 108, 500
- Charbonneau, P. 1995, *ApJS*, 101, 309
- Cochran, W. D., Endl, M., Wittenmyer, R. A., & Bean, J. L. 2007, *ApJ*, 665, 1407

- da Silva, L., et al. 2006, *A&A*, 458, 609
- Diego, F., Charalambous, A., Fish, A. C., & Walker, D. D. 1990, *Proc. Soc. Photo-Opt. Instr. Eng.*, 1235, 562
- Döllinger, M. P., Hatzes, A. P., Pasquini, L., et al. 2007, *A&A*, 472, 649
- Endl, M., Cochran, W. D., Kürster, M., Paulson, D. B., Wittenmyer, R. A., MacQueen, P. J., & Tull, R. G. 2006, *ApJ*, 649, 436
- Endl, M., Hatzes, A. P., Cochran, W. D., McArthur, B., Allende Prieto, C., Paulson, D. B., Guenther, E., & Bedalov, A. 2004, *ApJ*, 611, 1121
- Endl, M., Kürster, M., & Els, S. 2000, *A&A*, 362, 585
- Fischer, D. A., & Valenti, J. 2005, *ApJ*, 622, 1102
- Galland, F., Lagrange, A.-M., Udry, S., Chelli, A., Pepe, F., Queloz, D., Beuzit, J.-L., & Mayor, M. 2005, *A&A*, 443, 337
- Girardi, L., Bertelli, G., Bressan, A., Chiosi, C., Groenewegen, M. A. T., Marigo, P., Salasnich, B., & Weiss, A. 2002, *A&A*, 391, 195
- Gonzalez, G. 1999, *MNRAS*, 308, 447
- Gray, R. O., Corbally, C. J., Garrison, R. F., McFadden, M. T., Bubar, E. J., McGahee, C. E., O’Donoghue, A. A., & Knox, E. R. 2006, *AJ*, 132, 161
- Hatzes, A. P., Guenther, E. W., Endl, M., Cochran, W. D., Döllinger, M. P., & Bedalov, A. 2005, *A&A*, 437, 743
- Hekker, S., & Meléndez, J. 2007, *A&A*, 475, 1003
- Hekker, S., Reffert, S., Quirrenbach, A., Mitchell, D. S., Fischer, D. A., Marcy, G. W., & Butler, R. P. 2006, *A&A*, 454, 943
- Hekker, S., Snellen, I. A. G., Aerts, C., Quirrenbach, A., Reffert, S., & Mitchell, D. S. 2008, *A&A*, 480, 215
- Howard, A. W., et al. 2010, *Science*, 330, 653
- Jefferys, W. H., Fitzpatrick, M. J., & McArthur, B. E. 1987, *Celestial Mechanics*, 41, 39
- Johnson, J. A., et al. 2011, *AJ*, 141, 16

- Johnson, J. A., Aller, K. M., Howard, A. W., & Crepp, J. R. 2010a, *PASP*, 122, 905
- Johnson, J. A., et al. 2010c, *ApJ*, 721, L153
- Johnson, J. A., Howard, A. W., Bowler, B. P., Henry, G. W., Marcy, G. W., Wright, J. T., Fischer, D. A., & Isaacson, H. 2010b, *PASP*, 122, 701
- Johnson, J. A., et al. 2006, *ApJ*, 647, 600
- Johnson, J. A., Marcy, G. W., Fischer, D. A., Henry, G. W., Wright, J. T., Isaacson, H., & McCarthy, C. 2006, *ApJ*, 652, 1724
- Johnson, J. A. 2007, arXiv:0710.2904
- Johnson, J. A., et al. 2007, *ApJ*, 665, 785
- Kürster, M., Schmitt, J. H. M. M., Cutispoto, G., & Dennerl, K. 1997, *A&A*, 320, 831
- Marcy, G. W., Butler, R. P., Vogt, S. S., Fischer, D. A., Henry, G. W., Laughlin, G., Wright, J. T., & Johnson, J. A. 2005, *ApJ*, 619, 570
- Massarotti, A., Latham, D. W., Stefanik, R. P., & Fogel, J. 2008, *AJ*, 135, 209
- Murray, N., & Chaboyer, B. 2002, *ApJ*, 566, 442
- Niedzielski, A., Goździewski, K., Wolszczan, A., et al. 2009, *ApJ*, 693, 276
- O’Toole, S., et al. 2009, *ApJ*, 697, 1263
- O’Toole, S., et al. 2009, *ApJ*, 701, 1732
- Pasquini, L., Döllinger, M. P., Weiss, A., Girardi, L., Chavero, C., Hatzes, A. P., da Silva, L., & Setiawan, J. 2007, *A&A*, 473, 979
- Perryman, M. A. C., et al. 1997, *A&A*, 323, L49
- Saar, S. H., Butler, R. P., & Marcy, G. W. 1998, *ApJ*, 498, L153
- Sandage, A., Lubin, L. M., & VandenBerg, D. A. 2003, *PASP*, 115, 1187
- Sato, B., Kambe, E., Takeda, Y., Izumiura, H., Masuda, S., & Ando, H. 2005, *PASJ*, 57, 97
- Sato, B., et al. 2010, *PASJ*, 62, 1063
- Schuler, S. C., Kim, J. H., Tinker, M. C., Jr., et al. 2005, *ApJ*, 632, L131

- Setiawan, J., Pasquini, L., da Silva, L., von der Lühe, O., & Hatzes, A. 2003, *A&A*, 397, 1151
- Takeda, G., Ford, E. B., Sills, A., Rasio, F. A., Fischer, D. A., & Valenti, J. A. 2007, *ApJS*, 168, 297
- Tinney, C. G., Wittenmyer, R. A., Butler, R. P., Jones, H. R. A., O’Toole, S. J., Bailey, J. A., Carter, B. D., & Horner, J. 2011, *ApJ*, 732, 31
- Valenti, J. A., & Fischer, D. A. 2005, *ApJS*, 159, 141
- Valenti, J. A., & Fischer, D. A. 2008, *Physica Scripta Volume T*, 130, 014003
- Valenti, J. A., Butler, R. P. & Marcy, G. W. 1995, *PASP*, 107, 966.
- van Leeuwen, F. 2007, *A&A*, 474, 653
- Vogt, S. S., et al. 2010, *ApJ*, 708, 1366
- Wang, L., Liu, Y., Zhao, G., & Sato, B. 2011, *PASJ*, accepted.
- Wittenmyer, R. A., Tinney, C. G., Butler, R. P., O’Toole, S. J., Jones, H. R. A., Carter, B. D., Bailey, J., & Horner, J. 2011, *ApJ*, 738, 81
- Wright, J. T. 2005, *PASP*, 117, 657
- Wright, J. T., et al. 2011, *PASP*, 123, 412

Table 1. Pan-Pacific Planet Search Target List

Star	RA	Dec	<i>V</i>
224910	00 01 44.93	-16 31 54.2	7.83
749	00 11 38.06	-49 39 21.2	7.91
1817	00 22 21.22	-50 59 33.4	6.68
2643	00 29 54.99	-32 16 23.8	8.15
4145	00 43 50.09	-12 00 40.7	6.01
5676	00 58 12.43	-25 52 35.8	7.89
5877	00 59 19.25	-58 24 17.2	7.78
6037	01 01 38.60	-16 15 55.3	6.47
7931	01 18 32.20	-28 43 58.7	7.89
9218	01 30 13.84	-28 51 55.5	7.96
9925	01 35 43.11	-53 11 59.8	7.82
10731	01 43 28.25	-56 14 04.1	7.97
11343	01 50 06.22	-54 27 53.5	7.88
11653	01 53 00.51	-52 41 30.1	7.91
12974	02 06 56.07	-01 49 25.2	7.49
13471	02 10 54.48	-32 03 42.9	7.65
13652	02 12 34.49	-26 19 20.7	7.92
14805	02 20 43.08	-62 32 45.8	7.68
14791	02 22 07.00	-36 06 23.8	7.87
15414	02 26 12.48	-62 55 05.2	7.92
19810	03 10 51.47	-11 07 29.4	7.22
20035	03 11 57.63	-39 21 57.1	6.98
20924	03 21 58.79	-15 27 31.4	7.26
24316	03 51 32.65	-17 09 58.8	7.71
25069	03 58 52.42	-05 28 10.3	5.85
28901	04 32 06.76	-28 48 22.0	7.42
29399	04 33 34.10	-62 49 25.1	5.79
31860	04 57 46.42	-34 53 32.3	7.60
34851	05 12 02.21	-75 21 37.6	7.85
33844	05 12 36.08	-14 57 04.3	7.29
37763	05 31 52.66	-76 20 30.0	5.18
39281	05 48 34.16	-53 40 34.1	7.85
40409	05 54 05.90	-63 05 27.7	4.65
43429	06 15 17.71	-18 28 37.2	5.99
46262	06 20 53.87	-79 04 00.5	7.31
47141	06 36 05.42	-24 51 57.8	7.45
47205	06 36 41.00	-19 15 20.6	3.95
51268	06 53 33.56	-54 52 59.3	7.97
58540	07 22 57.03	-55 34 38.8	6.89
59663	07 25 09.11	-70 24 13.9	7.75
67644	08 06 20.28	-54 02 45.9	7.97
72467	08 32 01.89	-29 22 15.1	7.59
76321	08 54 57.73	-15 46 45.9	7.10
76437	08 55 01.65	-34 08 35.0	7.15
76920	08 55 16.78	-67 15 55.9	7.83

Table 1—Continued

Star	RA	Dec	<i>V</i>
80275	09 17 46.62	-35 41 23.8	7.70
81410	09 24 49.04	-23 49 34.4	7.35
84070	09 41 13.31	-46 22 55.1	7.88
85128	09 43 01.74	-79 35 30.2	7.30
85035	09 48 47.03	-19 18 48.6	7.02
87089	10 00 34.00	-61 45 31.3	7.93
86950	10 01 37.61	-17 19 58.8	7.47
HIP50638	10 20 33.31	-23 38 25.4	7.54
94386	10 53 32.86	-15 26 44.5	6.34
98516	11 19 47.64	-28 11 19.6	7.06
98579	11 20 19.05	-28 19 56.1	6.68
100939	11 36 48.17	-37 02 20.5	7.94
104358	12 01 00.72	-26 28 47.2	7.76
104704	12 03 22.27	-55 19 17.0	7.49
104819	12 04 11.05	-22 22 15.6	7.93
105096	12 06 01.36	-54 15 28.1	7.03
108991	12 31 38.47	-30 58 54.8	6.73
109866	12 38 49.98	-62 01 54.1	7.76
110238	12 40 59.85	-31 44 15.9	7.70
114899	13 14 26.28	-54 57 43.6	7.99
115066	13 15 04.35	-30 10 53.0	7.83
115202	13 15 58.58	-19 56 34.2	5.21
121056	13 53 52.27	-35 18 51.1	6.17
121156	13 54 16.75	-28 34 09.9	6.05
121930	13 59 46.00	-50 13 40.5	7.58
124087	14 11 45.85	-19 01 03.2	7.74
125774	14 21 49.23	-10 40 00.5	7.99
126105	14 24 00.33	-19 48 02.8	7.32
130048	14 46 13.51	-07 47 48.9	7.14
131182	14 52 21.07	-11 28 22.7	7.95
132396	15 00 00.35	-36 01 49.7	6.94
133166	15 04 36.20	-43 53 50.4	7.92
133670	15 06 27.10	-22 01 54.1	6.13
134443	15 11 31.92	-45 16 44.7	7.38
134692	15 14 59.90	-66 53 36.5	7.91
135760	15 18 17.43	-41 25 13.0	7.05
136295	15 20 41.44	-25 59 24.0	7.11
136905	15 23 26.06	-06 36 36.7	7.29
137115	15 24 57.58	-22 02 37.1	7.65
137164	15 27 45.75	-63 01 14.1	7.44
136135	15 27 47.09	-79 18 22.4	7.61
138061	15 29 59.95	-12 46 35.6	7.78
138716	15 34 10.52	-10 03 50.3	4.61
138973	15 36 08.23	-21 44 46.6	7.72
142132	15 54 24.55	-41 10 22.3	7.70

Table 1—Continued

Star	RA	Dec	V
142384	15 55 56.46	-40 47 11.0	7.41
143561	16 02 45.22	-42 30 25.5	7.97
144073	16 05 01.36	-26 56 52.0	7.60
145428	16 11 51.34	-25 53 00.3	7.73
148760	16 31 22.87	-26 32 15.2	6.07
153438	17 00 29.72	-21 27 41.3	7.35
153937	17 06 11.92	-60 25 14.8	7.43
154250	17 06 40.99	-48 00 43.5	7.96
155233	17 11 04.37	-20 39 15.2	6.81
154556	17 12 19.85	-70 43 15.2	6.21
159743	17 37 01.69	-18 59 30.9	7.45
162030	17 49 57.49	-24 12 25.1	7.02
166309	18 11 15.84	-29 38 22.4	7.61
166476	18 14 20.10	-58 42 20.9	7.81
170707	18 33 33.37	-50 12 41.5	7.75
170286	18 35 02.98	-71 19 26.1	7.72
173902	18 49 17.14	-34 44 56.0	6.59
175905	18 57 35.98	-00 31 34.6	7.66
176002	19 00 01.36	-43 20 49.7	7.92
175304	19 03 29.12	-76 06 54.8	7.75
177897	19 08 42.79	-45 04 34.3	7.74
176794	19 10 44.78	-76 24 15.7	6.94
181342	19 21 04.26	-23 37 10.2	7.55
181809	19 22 40.30	-20 38 33.6	6.72
188981	19 58 56.37	-30 32 17.7	6.27
191067	20 08 01.75	-00 40 40.9	5.97
196676	20 39 05.86	-04 55 46.2	6.46
199809	21 00 19.00	-27 20 35.9	7.93
200073	21 02 27.05	-38 31 50.0	5.93
201931	21 14 16.67	-45 46 57.2	6.89
204073	21 26 25.07	-12 05 42.0	6.70
204057	21 26 27.06	-15 14 42.9	7.97
204203	21 27 29.20	-20 12 45.2	7.84
205577	21 36 43.65	-21 30 09.8	7.93
205972	21 39 15.19	-13 53 41.0	7.25
205478	21 41 28.47	-77 23 22.1	3.73
208431	21 56 47.43	-28 49 03.3	7.91
208791	21 59 01.31	-11 17 03.4	7.79
214573	22 40 07.11	-49 35 53.2	7.37
215005	22 42 45.92	-37 20 43.7	7.93
216640	22 54 45.60	-16 16 18.3	5.53
216643	22 55 11.14	-46 40 43.9	7.53
218266	23 07 11.97	-45 50 33.2	7.92
219553	23 16 49.69	-21 12 10.7	7.25
222076	23 38 08.10	-70 54 12.3	7.47

Table 1—Continued

Star	RA	Dec	V
222768	23 43 32.71	-22 54 07.7	7.81
223301	23 48 28.19	-11 30 31.4	7.60
223860	23 53 13.59	-11 00 52.6	7.66

Table 2. Stellar Parameters for 7 CMa

Parameter	Value	Reference (m s^{-1})
Spec. Type	K1 III	Gray et al. (2006)
M_V	2.46 ± 0.03	da Silva et al. (2006)
$B - V$	1.037 ± 0.041	van Leeuwen (2007)
Mass (M_\odot)	1.52 ± 0.30	This work
	1.32 ± 0.12	da Silva et al. (2006)
Radius (R_\odot)	2.3 ± 0.1	This work
Luminosity (L_\odot)	11.3 ± 0.3	This work
Distance (pc)	19.75 ± 0.09	van Leeuwen (2007)
$V \sin i$ (km s^{-1})	1.15	Hekker & Meléndez (2007)
	1.0	Massarotti et al. (2008)
S_{MW}^a	0.132	Gray et al. (2006)
$[Fe/H]$	0.21 ± 0.10	This work
	0.18 ± 0.1	da Silva et al. (2006)
	0.21	Hekker & Meléndez (2007)
v_{micro} (km s^{-1})	1.32 ± 0.10	This work
	1.30	da Silva et al. (2006)
	1.45	Hekker & Meléndez (2007)
	1.0	Gray et al. (2006)
T_{eff} (K)	4792 ± 100	This work
	4744 ± 70	da Silva et al. (2006)
	4830	Hekker & Meléndez (2007)
	4799	Gray et al. (2006)
$\log g$	3.25 ± 0.10	This work
	3.11 ± 0.07	da Silva et al. (2006)
	3.40	Hekker & Meléndez (2007)
	3.05	Gray et al. (2006)

^aMount Wilson S-index

Table 3. 7 CMa Planetary Parameters

Parameter	Estimate
Period (days)	763±17
Eccentricity	0.14±0.06
ω (degrees)	12±41
K (m s^{-1})	44.9±4.0
T_0 (JD-2400000)	55520±89
$M \sin i$ (M_{Jup})	2.6±0.6
a (AU)	1.9±0.1
RMS of fit (m s^{-1})	7.5
N	21

Table 4. AAT Radial Velocities for 7 CMa

JD-2400000	Velocity (m s^{-1})	Uncertainty (m s^{-1})
54866.09800	24.11	5.73
54866.10107	17.47	5.86
54866.94000	1.93	5.81
54867.91576	-5.81	6.09
54869.08575	12.59	5.72
54871.03478	5.22	6.13
55140.18702	-42.28	5.56
55140.19229	-36.90	6.07
55227.06602	-37.51	5.82
55317.85529	-4.99	5.40
55317.85839	-9.87	5.33
55317.86143	-3.89	5.31
55495.13719	51.81	11.84
55525.22369	50.62	5.68
55526.21028	31.35	5.66
55581.09317	38.45	5.83
55601.00002	14.37	6.01
55670.87749	-10.70	13.99
55706.84304	-12.95	5.68
55783.30394	-43.20	5.85
55783.31112	-39.91	6.72

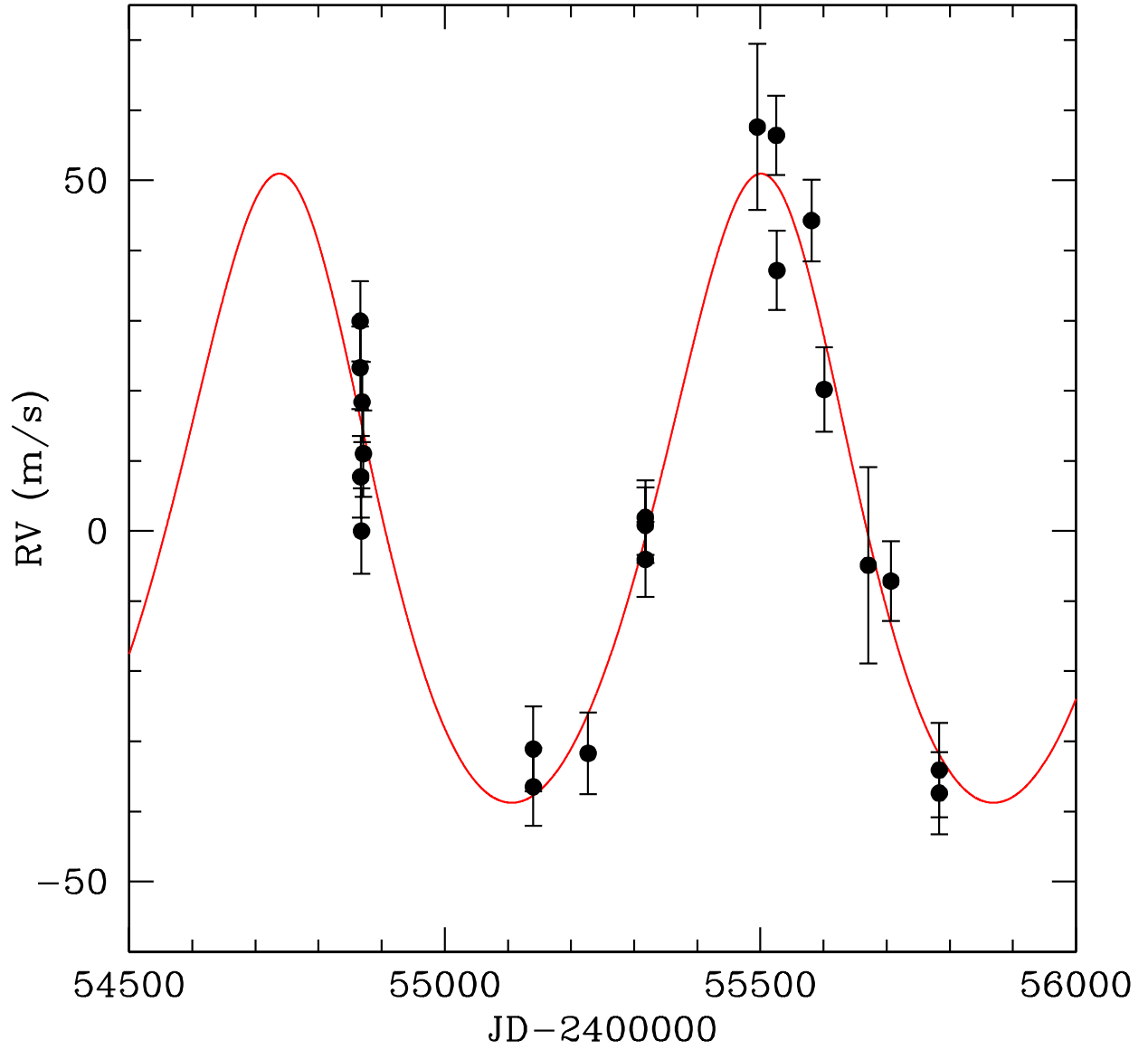


Fig. 1.— Radial-velocity data and Keplerian orbit fit for 7 CMA. The RMS scatter about the fit is 7.5 m s^{-1} , consistent with the mean uncertainty of 8.3 m s^{-1} (including 5 m s^{-1} of jitter added in quadrature).

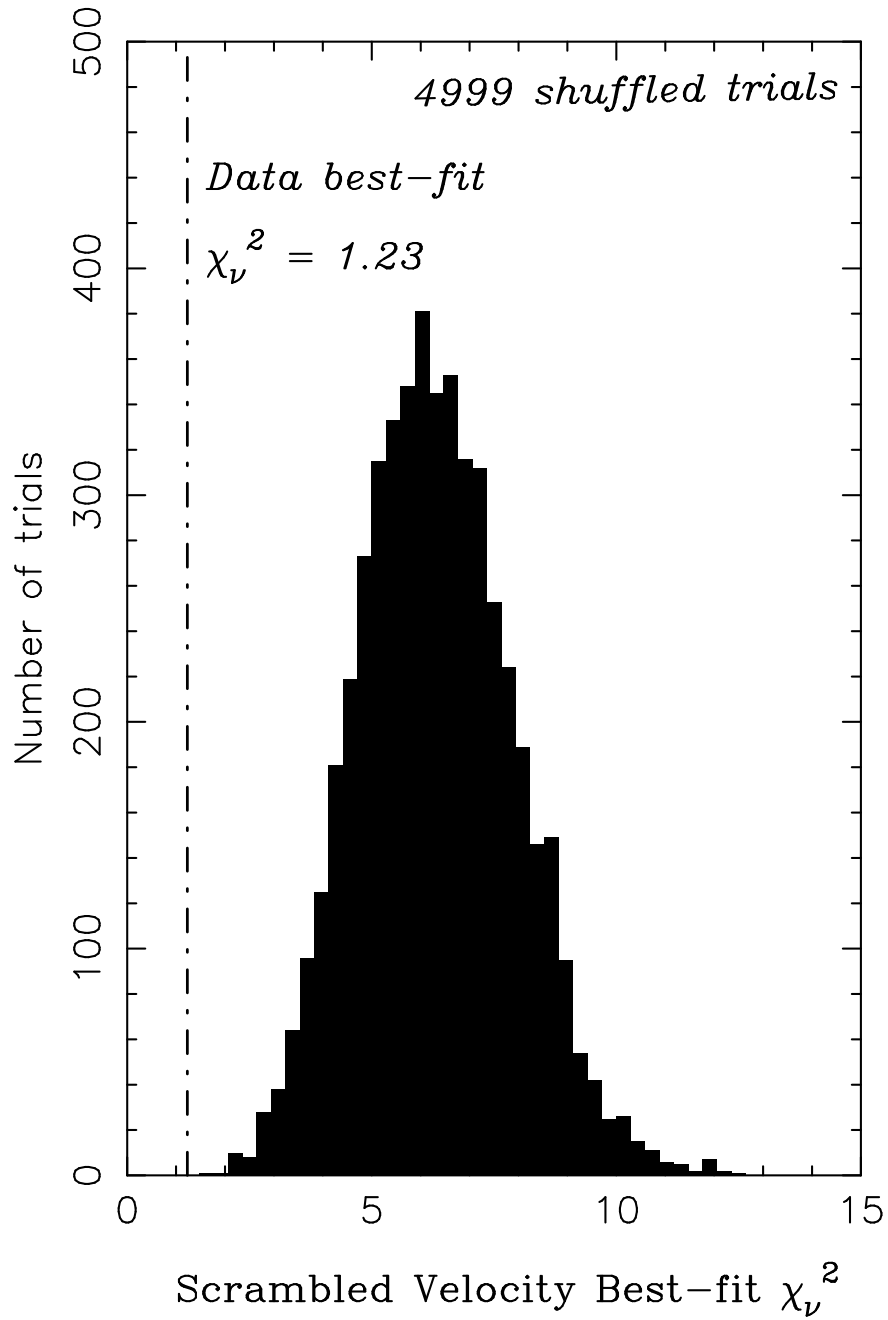


Fig. 2.— Results of 4999 trials in which the velocity data for 7 CMa were scrambled amongst the observation epochs. The reduced χ^2 of the original data is shown as a dashed vertical line. None of the scrambled data sets resulted in a better χ^2 , indicating a less than 0.02% chance that the observed variations are due to noise.

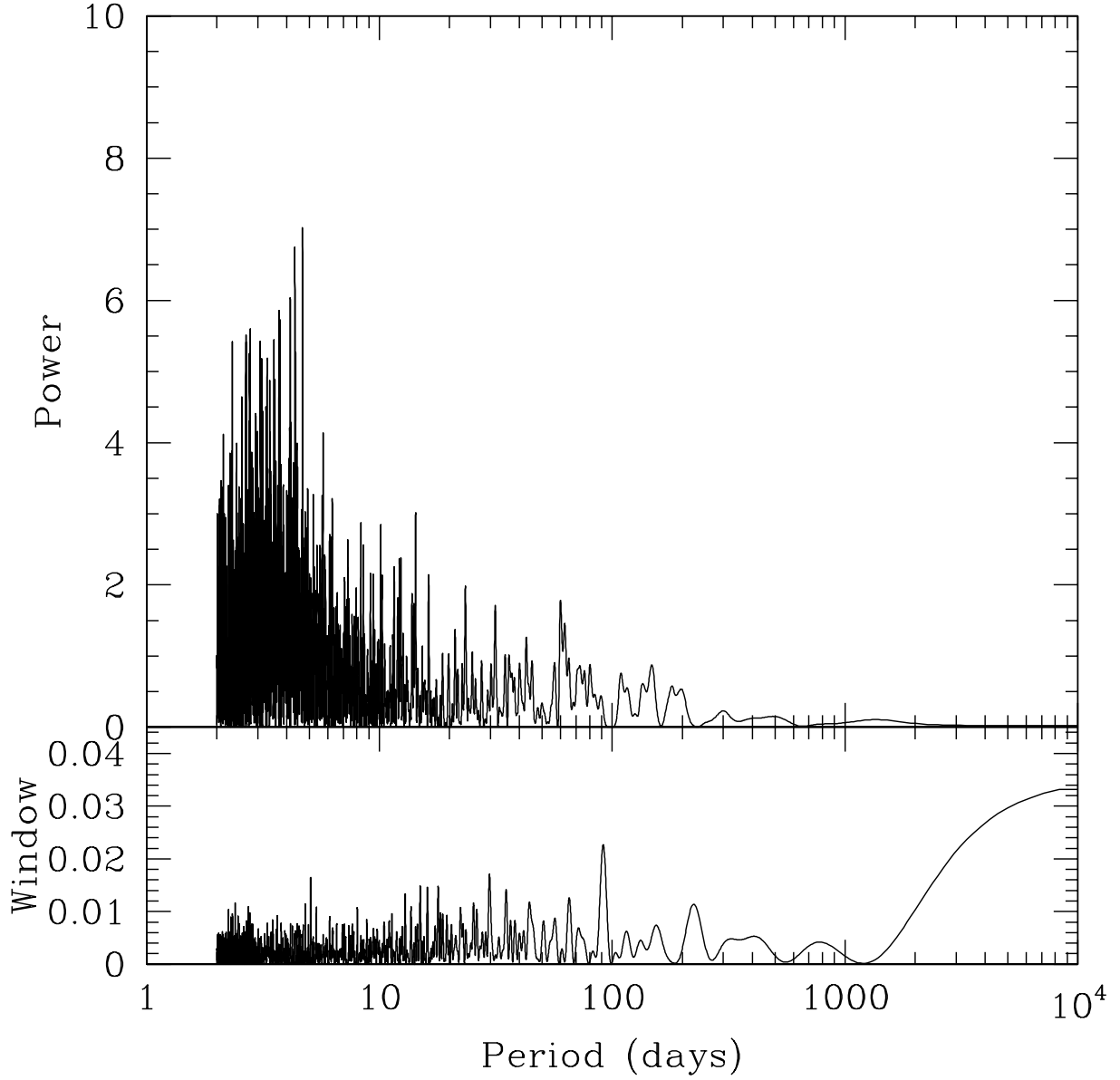


Fig. 3.— Periodogram of the residuals to the Keplerian orbit fit; no further signals are evident.

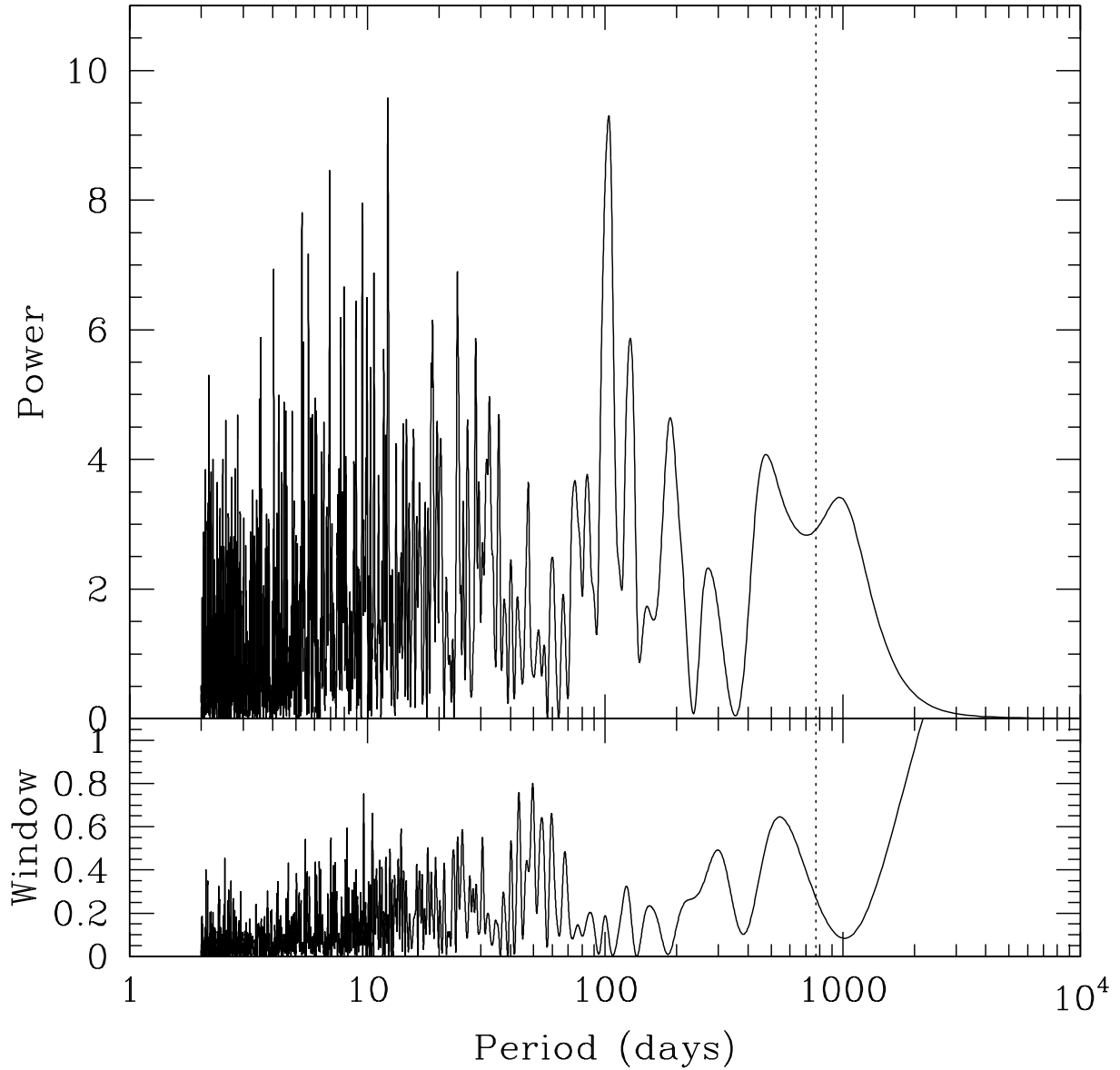


Fig. 4.— Periodogram of *Hipparcos* photometry for 7 CMa ($N = 168$). The two highest peaks are at periods of 12.2 and 103.7 days. The vertical dashed line indicates the 763-day period of the planet; there is no significant periodicity in the photometry near this period.

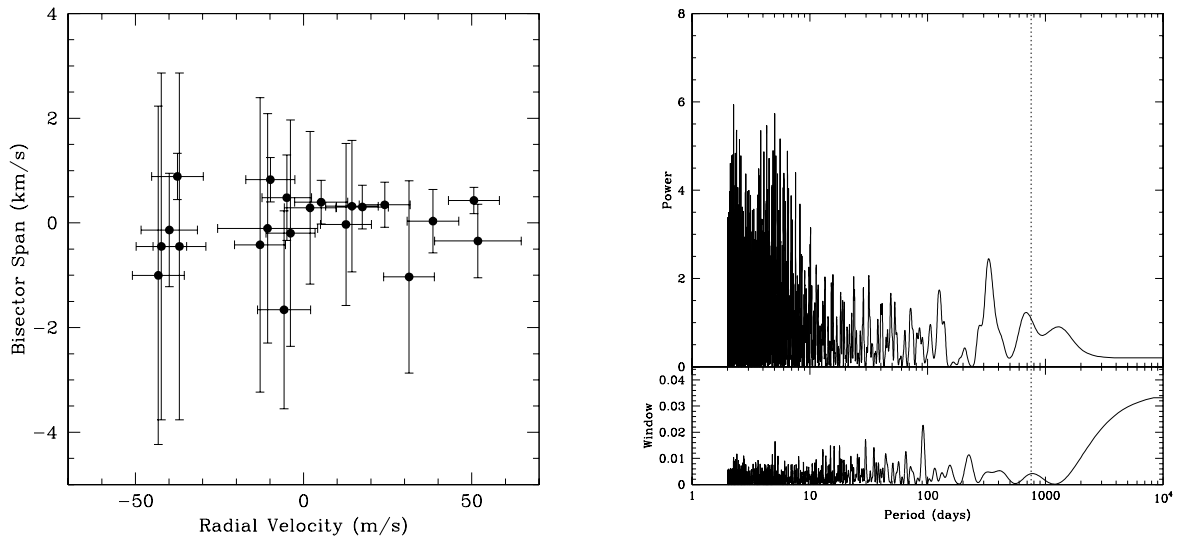


Fig. 5.— Left panel: Bisector velocity span versus radial velocity for the 21 observations for 7 CMa. A correlation would indicate that the observed radial-velocity variations were due to an intrinsic stellar process rather than an orbiting planet; no correlation is evident. Right panel: Periodogram of the bisector velocity spans. The vertical dashed line indicates the 763-day period of the planet; there is no significant periodicity near this period.

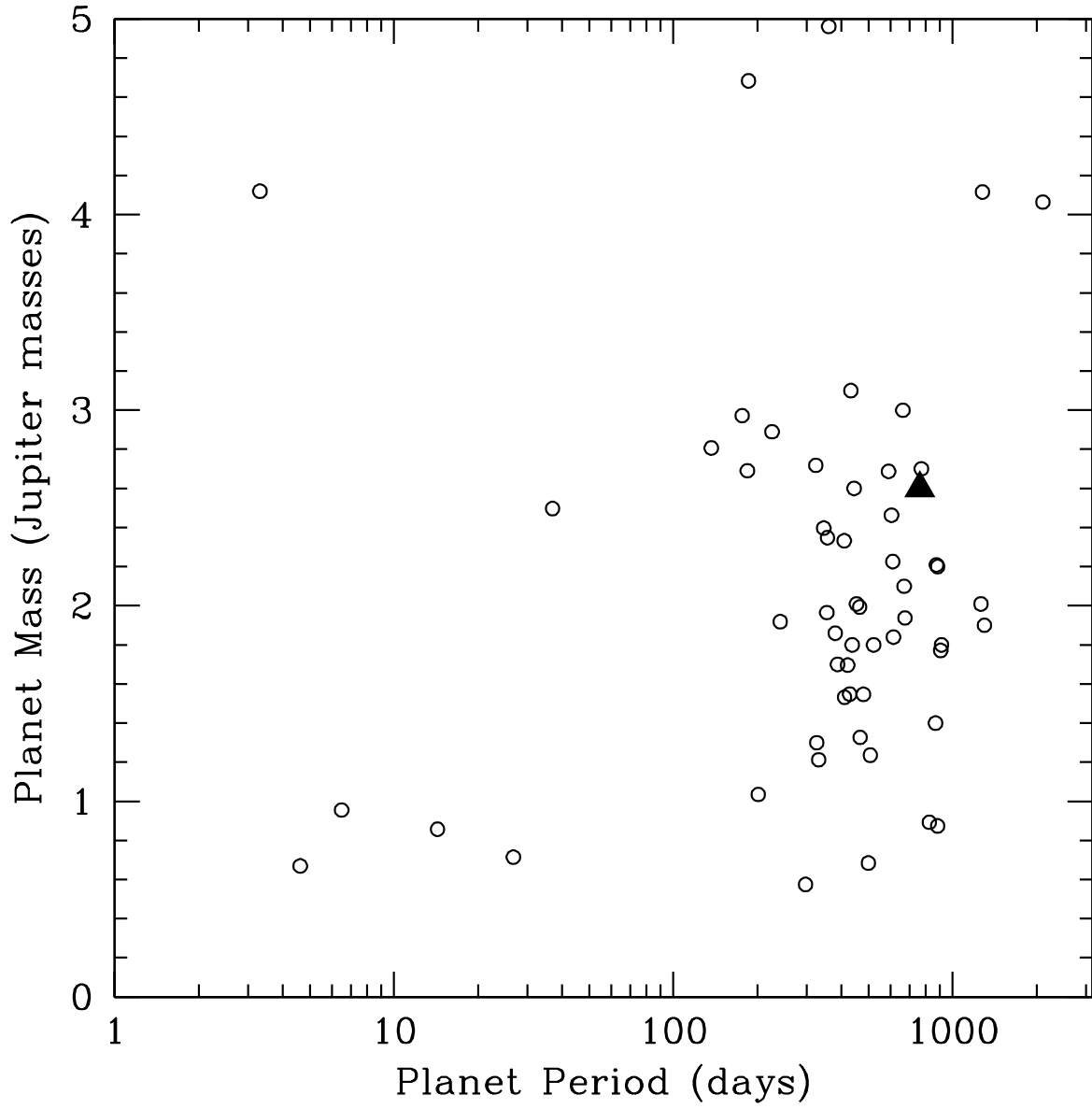


Fig. 6.— Mass-period plot for 83 radial-velocity detected planets orbiting stars with $M_* > 1.3 M_\odot$; planet data are from the Exoplanet Orbit Database (Wright et al. 2011). 7 CMa b is marked as a large filled triangle. Its parameters are consistent with other planets orbiting intermediate-mass stars.